Fusion Journal of Engineering and Sciences

Article

Integration of modal strain energy-based damage index and artificial neural networks for damage severity prediction in single-span steel bridges.

Zabeeh Ullah [1], Moazam Ahmed [1], Amir Ullah Khan[1], Ali Hussnain [1], Mehran Sahil [1], and Hafiz Ahmed Waqas [1*]

[1] Department of Civil Engineering, Ghulam Ishaq Khan Institute of Engineering Sciences and Technology, Topi 23460, Pakistan; zabeehafridi@gmail.com; moazamahmad17@gmail.com; iamirullah777@gmail.com; ali.063.husnain@gmail.com; mehransahil03@gmail.com; hafiz.waqas@giki.edu.pk
* Correspondence: hafiz.waqas@giki.edu.pk

Abstract

Structural health monitoring (SHM) is necessary to ensure durability and safety of steel bridges that are regarded as important elements of modern infrastructure. The structural integrity of bridges is very essential in order to keep them running and free of danger to the public. There has been a lot of research done on the prediction of damage locations in multi-span steel bridges, while relatively limited attention has been given to the identification and quantification of damage based on the level of severity in single-span steel bridges. This study provides an innovative method that integrates modal strain energy-based damage indices and data-driven artificial neural networks (ANNs) to provide damage localization and quantification in the form of damage severity in single-span steel bridges. The first two bending mode shapes obtained in the validated FE model were used to calculate the damage indices which was then combine using the absolute value method in determining the localization of damage in different damage scenarios created on the FE model. To predict the severity using these damage indices, ANNs were used with a large dataset created using cubic spline interpolations and FE simulations. This methodology reduces computational effort through a streamlined method for structural health monitoring while maintaining high accuracy in severity prediction and damage detection, enhancing infrastructure safety and maintenance.

Keywords: Finite Element Modeling; Modal Strain Energy-Based Damage Index; Damage Severity; Bending Modes; Artificial Neural Networks; Damage Detection.

1. Introduction

Bridges are a significant component of many infrastructures' development, and thus they are susceptible to easy destruction caused by alternate load characteristics, via wear and tear, earth tremors and impacts of weather conditions [1–7]. Damage can be observed in different bridge components, potentially leading to weakening and collapse of the structure. The safety of a bridge diminishes when defects in the structure become large, which means chances of a component-level or overall structural failures. Therefore, obtaining health of infrastructure, especially bridges, is become essential. Traditionally, bridge condition assessments have relied primarily on visual inspections, a nondestructive evaluation technique that is limited to detecting visible damage [5]. To prevent structural failures, structural health monitoring using smart techniques is necessary to assess structural damage at early stages However, utilizing recorded data to accurately estimate the location and severity of structural damage presents significant challenges.

Across the various techniques for damage detection, vibration-based methods (VBMs) have emerged as the most widely used and have gained significant attention in recent times. The principle of these methods is that damage alters the properties of a structure, such as stiffness, flexibility, damping, and mass, which consequently affect the dynamic parameters of the structure, such as natural frequencies and mode shapes [8–11]. The alteration in modal and structural properties serves as an indicator for detecting damage within the structure. The techniques based on these features are categorized into several types, such as curvature/strain mode shape-based methods, mode shape-based methods, natural frequency-based methods, and other techniques based on modal parameters [12]. In recent years, extensive research on damage identification has been carried out using VBMs across various structural elements and systems, including beams, trusses, plate structures, and bridges [13–19].

The modal strain energy (MSE) based DI one of the most effective techniques among all the VBMs. This method has been applied by many other researchers in order to identify the various kinds of damages. Originally it was provided by Kim and Stubbs applied to beam-like structure and this has been applied with success to detect and gauge the severity based on damage to steel girder bridges using the first three modes of vibration [20]. Their conclusion showed that it was possible to use the method of damage localization. In a similar study, Kim and Stubbs have suggested a better DI technique with unreliable constraints and assumptions resistant to current mathematical techniques of computation. This enhanced method was evaluated on a continuously supported two span beam and showed better localization of damages as well as assessing its severity. This enhanced method was evaluated on a continuously supported two span beam and showed better localization of damages as well as assessing its severity [21]. The results indicate that DI approach can be used in detecting damages in bridge girders.

Eraky et al. [22] use the DI technique to detect damage in flexural structural elements and indicated consistent reliable performance in the test work in terms of identifying all the simulated damage cases. All these studies imply that DI method is more effective in the detection of damage in flexural structures, which include bridge girders and decks. Consequently, it may be applied successfully to concrete bridges as well as to steel bridges with the purposes of damage detection. Shih et al. [23] evaluated the damage identification approach according to DI grounded on the mean square error (MSE) and modal flexibility in beams and plates. According to their results, the DI approach better offered plate structure accuracy. A generalized approach of detecting the damage in the plate structure based on pre and post damaged mode shapes was suggested by Cornwell et al. [14] that did not necessitate mass normalization and therefore efficient to identify the damage in case of ambient vibration. Their conclusion was that this method would be able to locate the damage that is related to a 10 % percent reduction in the stiffness. Samali et al. [24] have demonstrated the modal flexibility and DI approach on a timber bridge four-girder timber bridge and revealed that it could identify signs of severe and medium damages in either single or multiple damages cases, but not minor damages.

Cruz and Salgado assessed different vibration-based damage detection (VBDD) methods, including the DI method, on a reinforced concrete and composite bridge for identifying damage [25]. All methods successfully detected the damaged locations. Bonessio et al. [26] proposed a procedure for damage detection in seismically isolated bridges, utilizing VBDD techniques, which demonstrated consistent results in estimating severity and locating damage, with the DI method showing effectiveness in detecting damage in the bridge decks. Farrar and Jauregui employed the MSE-based DI method alongside four other VBDD methods to locate damage in a bridge featuring a steel girder [27]. Their findings indicated that the DI method achieved higher accuracy in damage detection when compared with conventional vibration-based techniques. Park et al. [28] assessed the correspondence between damage locations predicted by the DI method and those observed via visual inspection in a concrete box-girder bridge, demonstrating a strong correlation between observed and predicted damage locations.

Jayasundara et al. [29] proposed a dual index criterion incorporating the DI method, for detecting damage in structural components of deck-type arch bridges. Their approach demonstrated high accuracy in detecting damage in these bridges. Zhou et al. [30] assessed the effectiveness of five different damage detection techniques on the deck slab of a simply supported bridge two-girder bridge, focusing on detecting the location and magnitude of damage. Shih et al. [31] established a multi-criteria method for damage identification in slab-on-girder bridges, incorporating changes in MSE-based DI, modal flexibility, and natural frequencies, which successfully localized damage in all cases for both the girder and deck. The DI technique has also been applied to suspension bridges for damage detection. Talebinejad et al. [32] evaluated four different VBDD techniques, including the DI method, on a cable-stayed bridge, demonstrating that the DI method produces promising results compared to other VBDD techniques. Wickramasinghe et al. [33] proposed a DI method based on mode shape components to locate damage in pre-tensioned cables of a suspension bridge, finding that the DI method detected damage with reasonable accuracy. Despite the numerous benefits of VBDD methods, a significant limitation remains, as most of these techniques are unable to quantify the severity of the damage, although they are effective in locating and detecting damage.

Recently, the implementation of neural networks has garnered attention for structural damage identification. Artificial Neural Networks (ANN)**,** which can learn the mapping between inputs and outputs from training data, can be employed to quantify damage severities [34-35]. Lee and Yun presented a method for detecting damage in steel girder bridges using the DI method combined with back-propagation neural networks for locating and estimating damage severity, using mode shape properties as input features [36]. Their outcomes indicated that the damage severities estimated were subject to inaccuracies. Xu and Humar introduced a technique consisting of two stages that utilized the MSE-based DI for damage localization and an ANN for estimating severity in a girder-modeled bridge. In this approach, the DI was used as the input layer in the ANN and the results indicated that the ANN had the capability of predicting the damage severity especially where the damage was not minor [37].

Gu et al. [38] proposed a novel damage detection technique by incorporating an ANN to differentiate variations in natural frequencies due to damage induced by temperature variations. Tan et al. [39] introduced a two-stage procedure to localize damage in steel beams and estimate its severity.

Initially, the MSE-based DI was used for damage localization, followed by employing ANN training using DI as input parameters to predict damage magnitude. However, training the ANN required multiple damage scenarios involving calculations for all possible damage locations in the steel beam; for a complex structure such as a bridge, process becomes highly time-consuming. Mehrjoo et al. [35] introduced a neural network using back-propagation that utilized mode shapes and natural frequencies as input parameters to estimate the magnitude of damage in joints of a truss bridge. Their technique demonstrated that the limitation of trained ANN is that it could only predict the severity of single-damage scenarios. Bagchi et al. [40–41] used VBDD techniques and ANN on a three-dimensional finite element (FE) bridge model and a two-dimensional simple girder model for damage identification, using DI vectors as the input layer for the ANN. The accuracy of damage severity prediction was found to be low for small damage. Dackerman et al. [42] combined the MSE-based DI with principal component analysis and ANN to detect damage for single scenarios on a steel beam, using the input layer as the DI. The severity of damage could only be predicted when there was a single damage case. Hakim and Razak designed a methodology that input natural frequencies into the mapping of the ANN to identify the severity of the damage where the prediction error was 6.8% [43].

This study presents an improved two-step method of detecting and estimating the extent of damage in steel bridges. According to the literature study it is possible to say that MSE based DI method has proven to be accurate in localizing damage. In the first stage, the damage index (β) will be computed utilizing two initial bending modes. The indices that are acquired in the various modes are then merged together with the help of a data fusion process to generate only one plot depicting the trend between the damage index and the distance along the bridge girders, where peaks indicate the likely damage locations. In the second stage, the DI values corresponding to the identified damage locations are used to train an Artificial Neural Network (ANN), which is subsequently employed to estimate the severity of damage for single-damage scenarios.

The Alamosa Canyon Bridge is utilized as a sample structure to examine the feasibility of the methodology proposed, with a model and description of the bridge provided along with the validation of the FE model. Subsequently, various damage scenarios are introduced to the sample structure by reducing the stiffness of specific members, and application of these defined damage cases were carried out on the validated FE model. The proposed damage detection technique is then employed to detect the location and estimate the severity or quantify the severity of the damage, and the results are interpreted in the conclusion section of this paper. The methodological framework of the current research is illustrated in Figure 1.

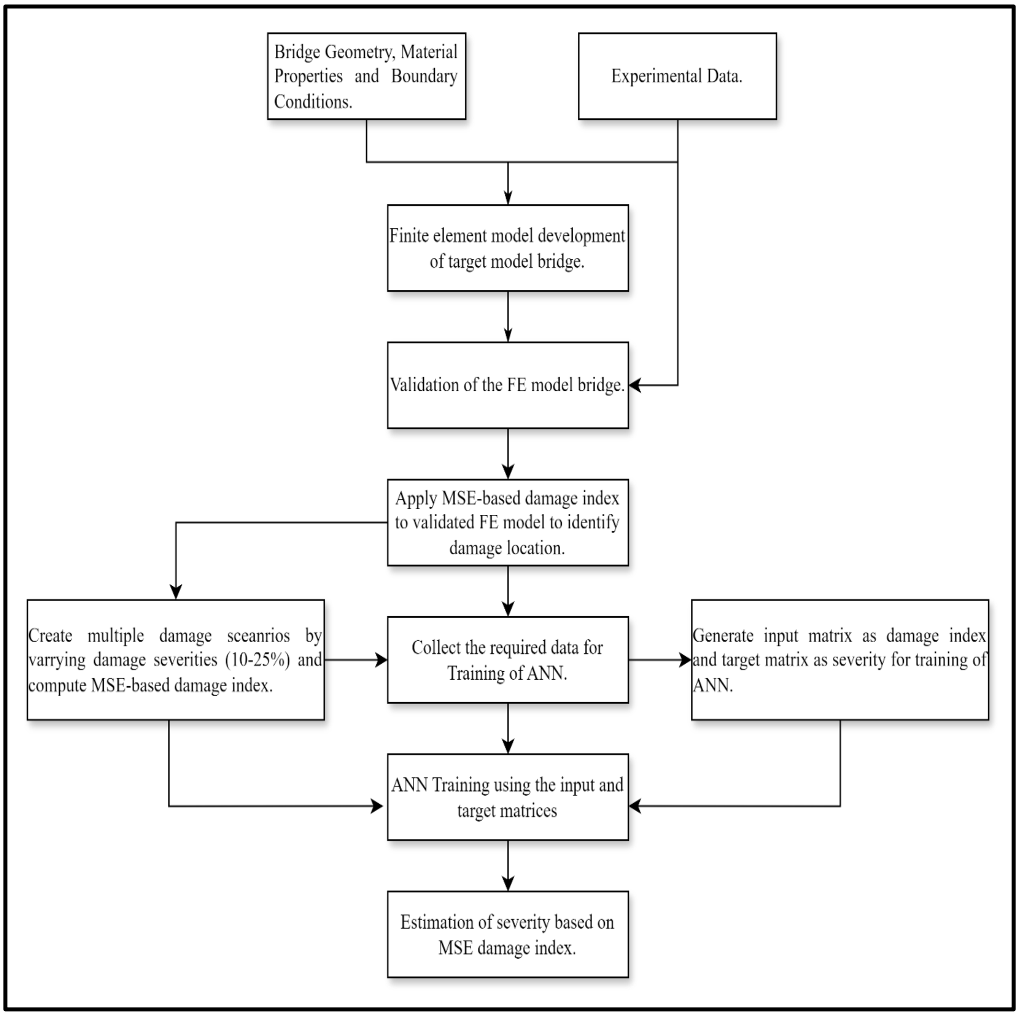

Figure 1: The current study methodological flow chart.

2. Materials and Methods

2.1 Bridge Description and Material Properties

In Sierra County, New Mexico, USA, the Alamosa Canyon Bridge shown in Figure 2, —constructed from reinforced concrete and steel and facilitating transportation across Alamosa Canyon—was selected as the target bridge for this study [44]. Preliminary experimental vibration tests were conducted on the bridge to estimate its dynamic characteristics, such as natural frequencies and mode shapes. A finite element (FE) model of the Alamosa Canyon Bridge, was utilized to evaluate the damage detection capability.

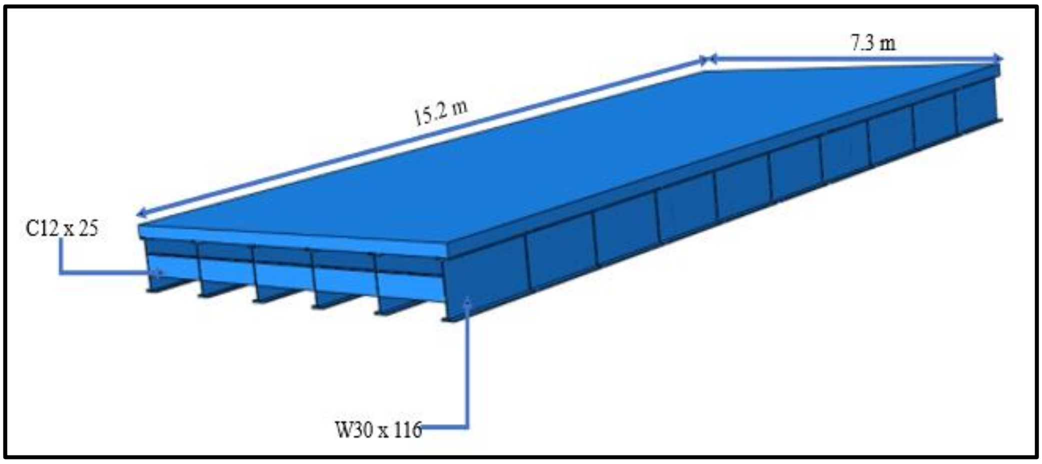

Figure 2 : FE model of Alamosa Canyon bridge.

The material properties used for the steel and concrete are presented in Table 1. This bridge consists of seven spans, each connected through expansion joints and bridge piers, allowing for independent structural analysis of each span. It features a concrete deck supported by six W30 × 116 steel beams, with each span having a roadway width of 7.3 meters (24 feet) and a length of 15.2 meters (50 feet), including expansion joints at both ends. Additionally, each span is equipped with four equally spaced C12 × 25 channel-section cross braces connecting the adjacent beams.

Table 1: Material properties for steel and concrete.

Details	**Mass Density (kg/m^3)**	**Elastic Modulus (GPa)**
Steel	7850	200
Concrete	2400	21

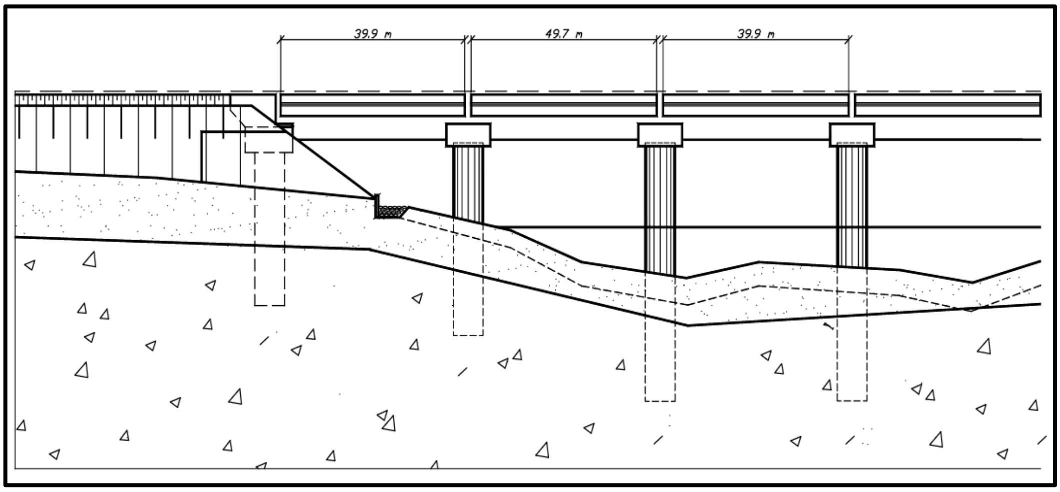

Figure 3 : Bridge section view (up to damage part)

2.2 Boundary Conditions, Meshing, and Interactions

The Alamosa Canyon Bridge was modeled using the FE modeling tool Abaqus (2020), and the numerical model of the bridge is illustrated in Figure 2. The influence on eigenvalue results due to boundary condition assumptions was examined, based on the fact that real-world boundary conditions often deviate from idealized representations. To account for this, minor agitations were introduced to the boundary constraints through a sensitivity analysis, such as variations in fixity and restraint conditions. The resulting changes in the computed eigenfrequencies were observed to be marginal, suggesting that the model exhibits satisfactory results despite boundary condition variations. As shown in Figure 3, the bridge's support conditions were modeled using pinned and roller-type bearings, consistent with previous studies. Specifically, the left side of the FE model was represented as a pinned boundary condition, and the right side was modeled as a roller boundary condition.

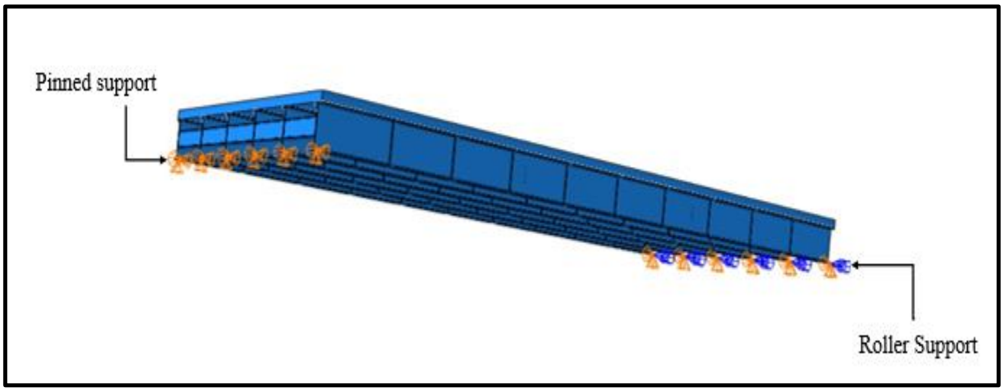

Figure 4: Support condition of the FE model bridge.

The FE model employed Continuum 3-dimensional 8-node (C3D8) solid brick elements to represent the bridge deck, girders, and cross braces. A mesh convergence analysis was also carried out in order to have a reliable outcome of the simulation. This study involved the incremental refinement of the finite element mesh and computing the corresponding eigenvalues at each refinement level. The refinement process was continued until the relative difference in the primary natural frequencies between successive mesh configurations fell below a threshold of 1%, indicating convergence. The mesh size adopted for the final simulations was selected as the optimal balance between numerical accuracy and computational efficiency.

The meshed view of the bridge is represented in Figure 4, which illustrates the mesh of each element. To optimize the model, a coarser mesh size was assigned to the deck elements, while a finer mesh size was applied to the main girders and cross braces, in line with prior research recommendations, which suggest maintaining the mesh size at approximately four to five times the thickness of the respective member [45]. For interactions, the members of the FE model were interconnected using tie connections to ensure an accurate simulation of the bridge's structural behavior.

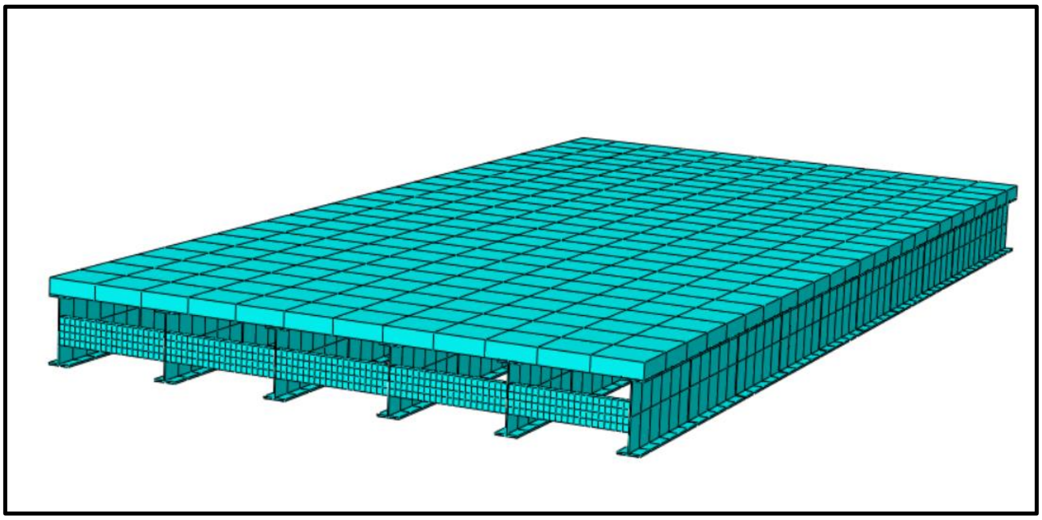

Figure 5: Meshed geometrical view of FE model bridge.

2.3 MSE-Based Damage Index

An approach based on determining the strain energy produced within damaged elements of beam for a specific mode shape was developed by Kim and Stubbs [20]. This approach serves as a guide for damage detection in structural elements. The mathematical equation for strain energy in a beam is presented in Equation (1).

$$\mathrm{U} = \int_0^L \frac{EI}{2}\left(\frac{\mathrm{d}^2 w}{\mathrm{d}x^2}\right)\mathrm{d}x \tag{1}$$

The mathematical expression includes key terms such as flexural rigidity (*EI)*, beam span (*L),* curvature($\frac{d^2 w}{dx^2}$), while *x* indicates the span determined along the length, and *w* denotes the vertical deformation of the damaged beam. The beta index is decided using the variations relative to the MSE against the undamaged and damaged position of a structure. The damage index β_{ij} for the ith mode of the jth beam element is stated in the below Equation (2).

$$\beta_{ij} = \frac{\int_j^* [\emptyset''^*{}_i\,(x)]^2 \mathrm{d}x + \int_0^L [\emptyset''^*{}_i\,(x)]^2\ \mathrm{d}x)\int_0^L [\emptyset''{}_i\,(x)]^2 \mathrm{d}x}{\int_j^* [\emptyset''{}_i\,(x)]^2 \mathrm{d}x + \int_0^L [\emptyset''{}_i\,(x)]^2\ \mathrm{d}x)\int_0^L [\emptyset''^*{}_i\,(x)]^2 \mathrm{d}x} \tag{2}$$

The * indicates the damaged state, and $\emptyset_i''$ is the curvature based on mode shape, as per the Expression above, and can be written as follows:

$$\beta_{ij} = \frac{[(\emptyset''^*{}_{ji})^2 + \Sigma(\emptyset''^*{}_{ji})^2]\,[\Sigma(\emptyset''{}_{ji})]^2}{[(\emptyset''{}_{ji})^2 + \Sigma(\emptyset''{}_{ji})^2]\,[\Sigma(\emptyset''^*{}_{ji})]^2} \tag{3}$$

To account for all the existing modes, a separate damage indicator β_j is produced for N number of modes as given in the below Equation (4), where Num_{ji} and Denom_{ji} denote the numerator and denominator of β_{ij} from Equation (3).

$$\beta_j = \frac{\sum_{i=1}^N \mathrm{Num}_{ji}}{\sum_{i=1}^N \mathrm{Denom}_{ji}} \tag{4}$$

For damage-based detection, it is proposed to calculate the DI for each bending mode separately using Equation (3) and then combine them using the absolute value method to incorporate both bending modes of the target FE bridge. Using the AV method, the normalized combined damage indices are defined by Equation (5).

$$\beta_{AV} = \frac{\sum_{i=1}^{m} |\beta_j|}{M}$$

(5)

The β_j represents the DI calculated from the modal information of each of the bending modes, and M denotes the number of calculated damage indices.

2.4 Artificial Neural Networks (ANN)

ANN were initially created to match the human brain's functionality, and are employed in this methodology to assess severity based on damage. These types of networks have the ability to learn as well and are specifically adaptive to complicated logical processes [43]. Every ANN consists of three layers; an input and an output layer and multiple hidden layers. The interaction between the input and output layer may be linear or nonlinear which depends on a set of constraints such as bias vectors and weight matrices The multilayer perceptron (MLP), usually implemented as a back-propagation neural network (BPNN), is one of the most used ANN algorithms trained using supervised learning in the field of structural health monitoring (SHM). This study utilizes the BPNN algorithm to compute weight matrices required to develop the anticipated pattern of input parameters versus output parameters. Back-propagation is the method of passing data in the forward direction whereas the error propagation is carried out backwards in the network until an optimal point is reached. The performance index is the least mean square error that the BP algorithm utilizes and that is the difference between what the network output and the output parameters. In this methodology, the Levenberg-Marquardt BP method, available in MATLAB software, was used to establish the relationship between MSE-based DI and severity-based damage as output parameters.

The architecture of ANN model is shown in Figure 5, designed for a regression task to predict "Severity" based on the 'Beta' value. LSTMs are typically designed for time-series data, they were used here to model complex non-linear relationships in the static Beta Severity mapping, even without explicit temporal dependencies. This approach utilized the LSTM's ability to capture intricate patterns and feature interactions beyond what simpler models might detect. Although the dataset comprises static DI values, the use of LSTM was a deliberate architectural choice to explore its pattern recognition strengths. The input layer has a shape of (1, 1), as each sample consists of one-time step and one feature, the 'Beta' value. The first layer is an LSTM layer with 64 neurons (units), and L2 regularization (0.001) is applied to both kernel and recurrent weights. The LSTM layer uses tanh as the activation function for the outputs and sigmoid for the gates. The second layer is a Dense (fully connected) layer with 32 neurons, applying L2 regularization (0.001) to the weights and using a linear activation function. The output layer consists of one neuron, with a linear activation function, appropriate for the regression task. For training, the model uses the Adam optimizer with a learning rate of 0.01. The loss function is Mean Squared Error (MSE), and the performance is monitored using the Mean Absolute Error (MAE) metric. The model is trained for 300 epochs with a batch size of 32, and 20% of the training data is used for validation. L2 regularization is applied throughout the model to reduce overfitting, and the architecture is optimized for accurate regression predictions.

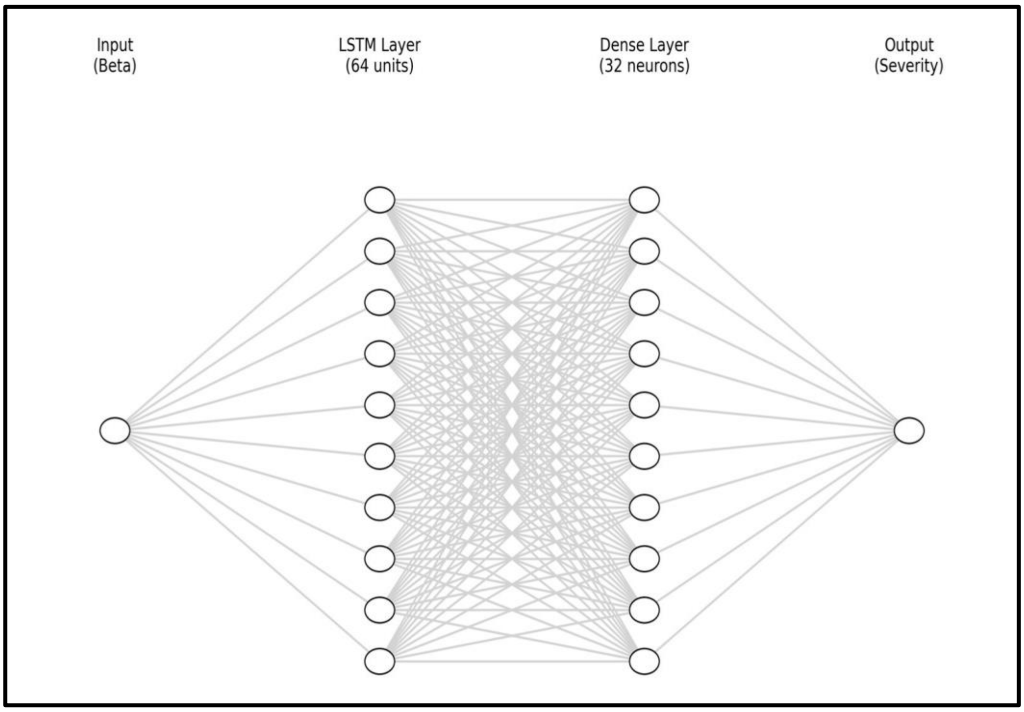

Figure 6: Neural Network Architecture

2.5 Validation of FE Model

The forced vibration test technique was utilized to extract the modal parameters and validate the finite element (FE) model by comparing the frequencies derived from the undamaged structure with the experimental resonant frequencies. For this validation, as presented in Table 2, resonant frequencies calculated via FE analysis were compared with those obtained through experimental testing on the actual bridge.

Table 2: Comparison of natural frequencies of the bridge from experiment and FE analysis.

Mode	**Experiment** [44]	**FE model**	**Average percentage difference**
1st	7.81	7.18	8.43
2nd	8.51	9.36	
3rd	12.1	15.85	
4th	20.80	21.04	
5th	24.00	24.77	
6th	26.60	25.32	

The forced vibration test technique was utilized to extract the modal parameters and validate the finite element (FE) model by comparing the frequencies derived from the undamaged structure with the experimental resonant frequencies. For this validation, as presented in Table 2, resonant frequencies calculated via FE analysis were compared with those obtained through experimental testing on the actual bridge.

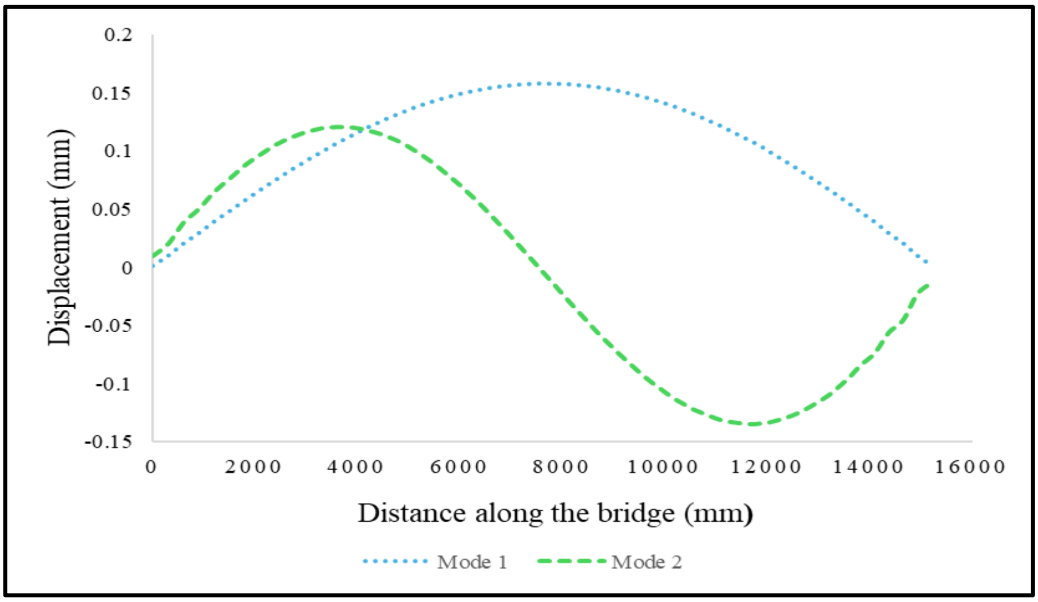

Figure 7: First two bending modes of the undamaged bridge.

2.6 Damage Detection and Severity Prediction Approach

This study focuses on identifying damage in the Alamosa Canyon Bridge using an FE model and various damage scenarios, followed by predicting the severity of the damage. The validated FE model underwent a damage identification process to demonstrate the effectiveness of the proposed damage detection technique. The FE model featured a single span supported by six steel beams, each divided into nine segments of 30 mm length along the span, representing potential damage locations. Damage was simulated by a 10% reduction in elastic modulus for a specific damage scenario, and a frequency analysis of the numerical model was conducted to extract the first two bending mode shapes of the Alamosa Canyon Bridge. The central difference technique was then applied to these mode shapes to compute the damage index at specific damage locations, utilizing Equations (3) and (4). The absolute value (AV) method was used to combine these indices as described in Equation (5), and the computed absolute damage indicators were plotted along the span of the bridge to visually identify the damage location.

As stated in Table 3, various damage severities for all damage cases were initially simulated in the FE model at the damage locations to gather learning data for the ANN. After simulating multiple damage scenarios on the FE model bridge, the next phase involved training an ANN. To reduce computational costs, an efficient method was proposed to interpolate damage indices instead of calculating them for all severities. The ANN was trained using these damage indices as input parameters. The damage indices were calculated for four different severities (10%, 15%, 20%, and 25%), and interpolation for the remaining damage magnitudes was carried out using the cubic spline method in Microsoft Excel.

Table 3: Damage scenarios simulated on the FE model bridge.

Scenario	Location	Damage Severities (%)
Case 1	Center	10 - 15 – 20 - 25
Case 2	Left middle third	10 - 15 – 20 - 25
Case 3	Right middle third	10 - 15 – 20 - 25

The proposed methodology for damage detection and severity prediction in the Alamosa Canyon Bridge follows a systematic sequence. Initially, a finite element (FE) model was developed using target bridge, incorporating accurate geometric and material properties of the bridge. A mesh convergence study was conducted to ensure computational reliability. Modal analysis was then carried out to extract the first two bending mode shapes, which were used to compute modal strain energy-based DI through the absolute value method. Various damage scenarios were simulated by reducing the elastic modulus, and the corresponding DIs were calculated. To estimate damage severity, a supervised artificial neural network (ANN) model—incorporating a Long Short-Term Memory (LSTM) architecture—was trained using the computed DI. Additional severity levels were interpolated using the cubic spline method to enhance the training dataset. The FE model was validated against experimental vibration data to ensure reliability of the simulation results.

3. Results

3.1 Damage Location Detection

The performance of the method in detecting specific damage in the first stage is demonstrated by its application to a damaged case. Firstly, using the first two bending modes, the damage location is determined using the MSE-based damage indicator for each damage scenario. The first two bending modes of the bridge are used to calculate the β_{AV}, and it is plotted across the length of the target bridge. The expected indication of damage locations comes from observing the DI peaks in these plots. Figures 6 to 8 depict bar charts displaying the absolute damage index plotted against the distance along the bridge for each scenario of damage with 10% severity. Figures 9 to 11 depict charts displaying the absolute damage index plotted against the distance along the bridge for all damage cases described in Table 3. These charts further support the accuracy of the damage detection procedure, as they successfully pinpoint the damage at the actual locations. These damage indices were calculated using data obtained from the first two bending modes.

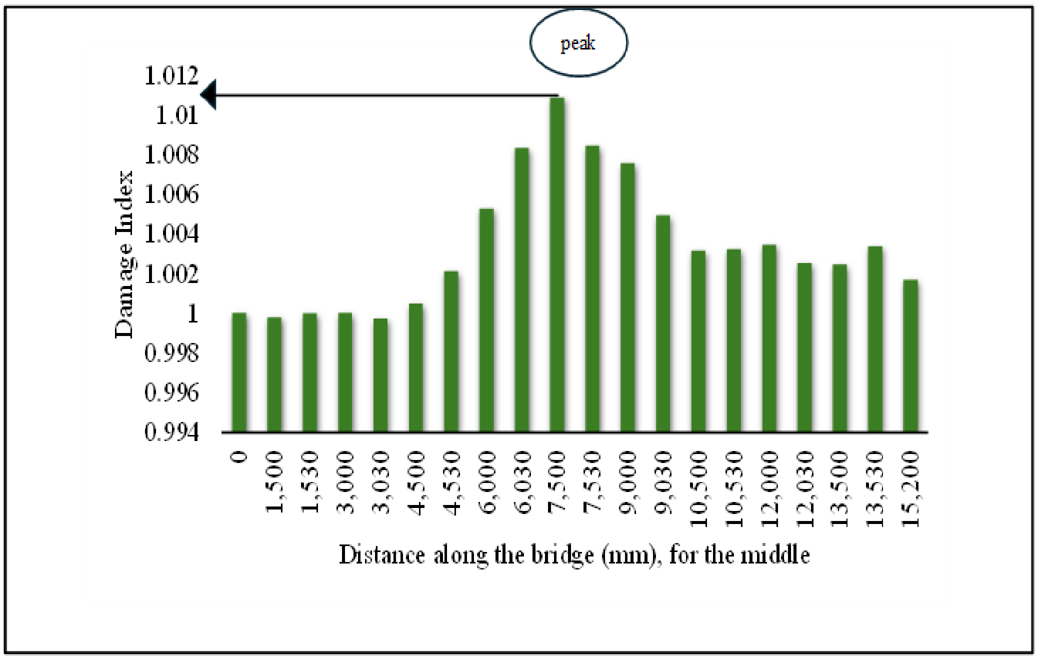

Figure 8: Absolute damage index versus distance along the bridge for 10% severity.

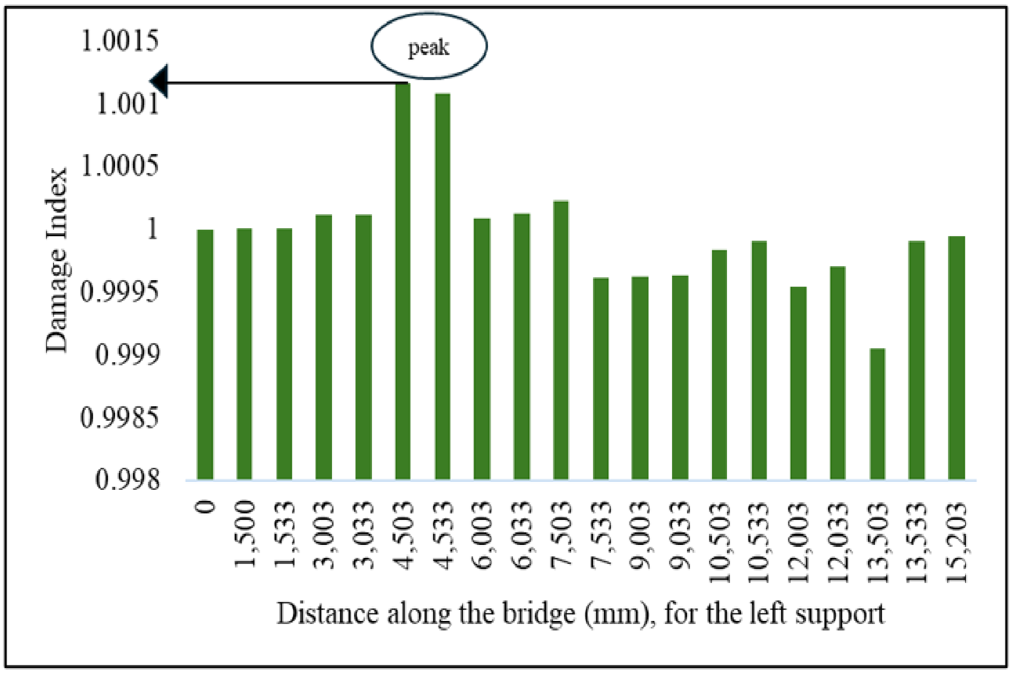

Figure 9: Absolute damage index versus distance along the bridge for 10% severity.

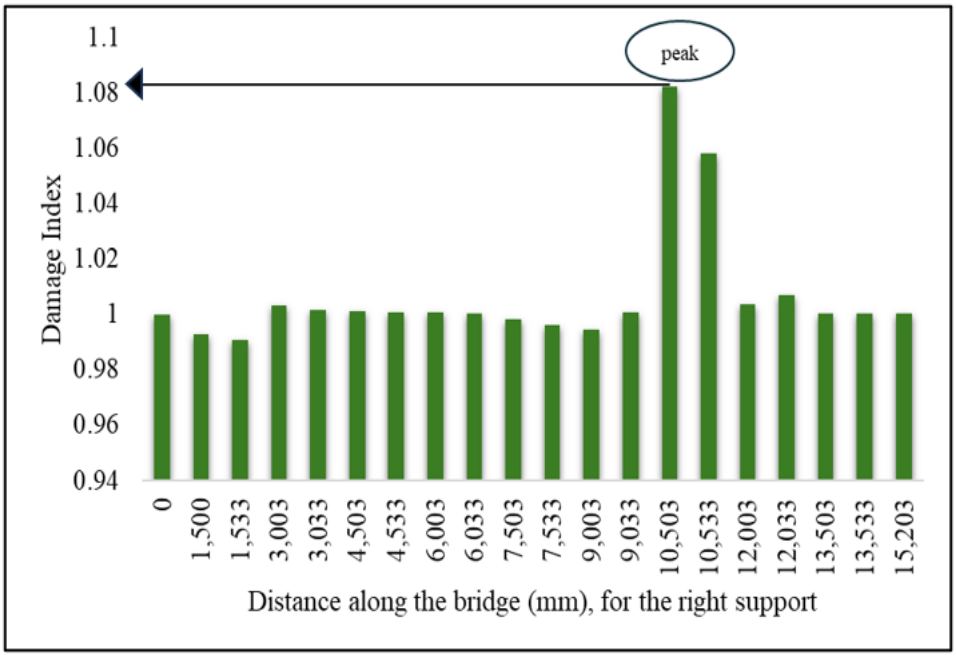

Figure 10: Absolute damage index versus distance along the bridge for 10% severity.

The above figures demonstrate the accuracy of the MSE-based DI in identifying damage for various scenarios at different locations. The use of the MSE-based DI is validated through its ability to detect and locate structural damage accurately across multiple scenarios, as depicted in the figures. Figure 6 illustrates damage occurring at the center of the bridge, with a peak observed precisely at this central point**.** In Figure 6, the damage detection results highlight an evident peak at the center of the bridge, indicating the exact location of the damage. Similarly, Figures 7 and 8 accurately pinpoint damage locations, with peaks concentrated in the right-middle third and left-middle third regions for each damage scenario. Figures 7 and 8 further validate the effectiveness of the MSE-based DI by showing distinct peaks in the right-middle third and left-middle third sections of the bridge. These peaks align with the predefined damage scenarios, demonstrating the method's capability to locate damage with precision in different regions of the bridge structure.

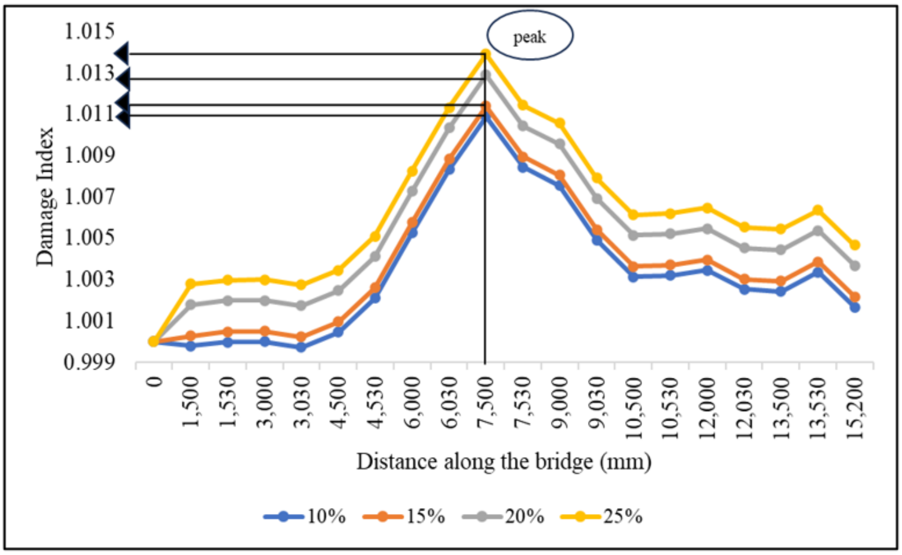

Figure 11: Damage index vs Distance along the bridge for case 1.

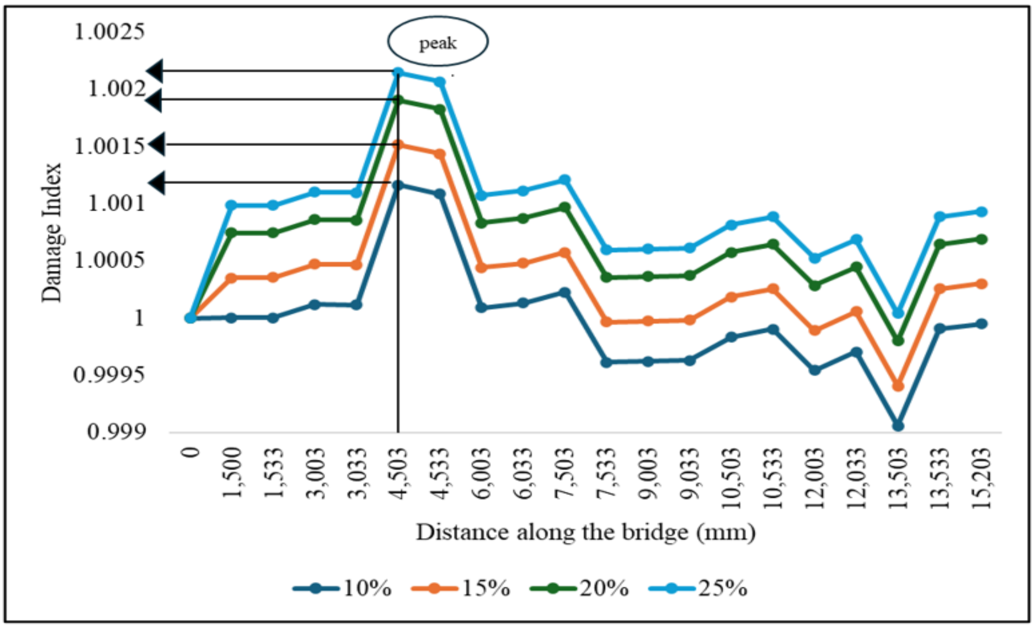

Figure 12: Damage index vs Distance along the bridge for case 2.

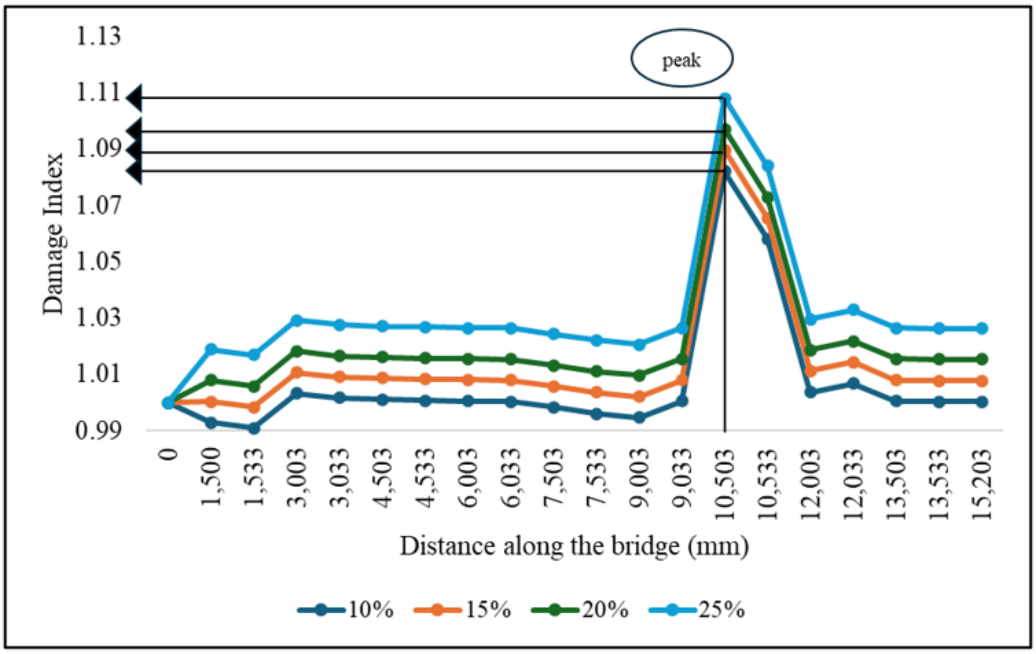

Figure 13: Damage index vs Distance along the bridge for case 3.

The charts presented in Figures 9 to 11 illustrate the relationship between the DI and span length for various damage severities, ranging from 10% to 25%. In Figure 9, which represents damage scenario 1, damage is consistently detected at the center of the span for all severities. As the severity of the damage increases, the identification becomes more pronounced, with the peaks indicating damage becoming more prominent and higher compared to those of lower severities. Similarly, Figures 10 and 11 accurately pinpoint the damage locations in the right-middle third and left-middle third regions of the bridge, respectively. The charts show that as the severity of the damage increases, the absolute values of the damage index also increase, enhancing the visibility and accuracy of the damage detection. Overall, these results demonstrate high accuracy in determining the damage locations for all scenarios and severities, validating the effectiveness of the proposed damage detection method. This consistent pattern across different figures underscores the reliability of the MSE-based DI employed in accurately identifying and assessing damage in the bridge structure.

3.2 Prediction of damage severity

The proposed methodology was further employed to assess the efficacy of mode shapes in estimating damage severity. As observed in the preceding analysis, the damage detection methodology accurately identified damage. To investigate the severity at the damage location, an ANN was trained with the data sets created using the damage scenarios stated in Table 3. Since ANN requires more learning data, the data sets were enhanced by applying cubic spline interpolation to the data extracted from the FE model. To evaluate the accuracy of the cubic spline interpolation method, Table 4 and Figure 12 show the actual and interpolated data for the existing four severities using cubic spline interpolation in Microsoft Excel, along with the percentage difference between the extracted and interpolated data. The beta vector for four different damage severities was initially assessed at the location of damage 1, and subsequently, the damage indices for 15% and 20% reductions in stiffness were interpolated using the technique of cubic spline.

Table 4 : Comparison of computed and interpolated damage index.

Damage Severity	Damage index	Interpolated damage index	Percentage Difference (%)
10	1.010892557	1.010892557	
15	1.011392557	1.011892557	0.000494124
20	1.012192557	1.012892557	0.00069109
25	1.013892557	1.013892557	

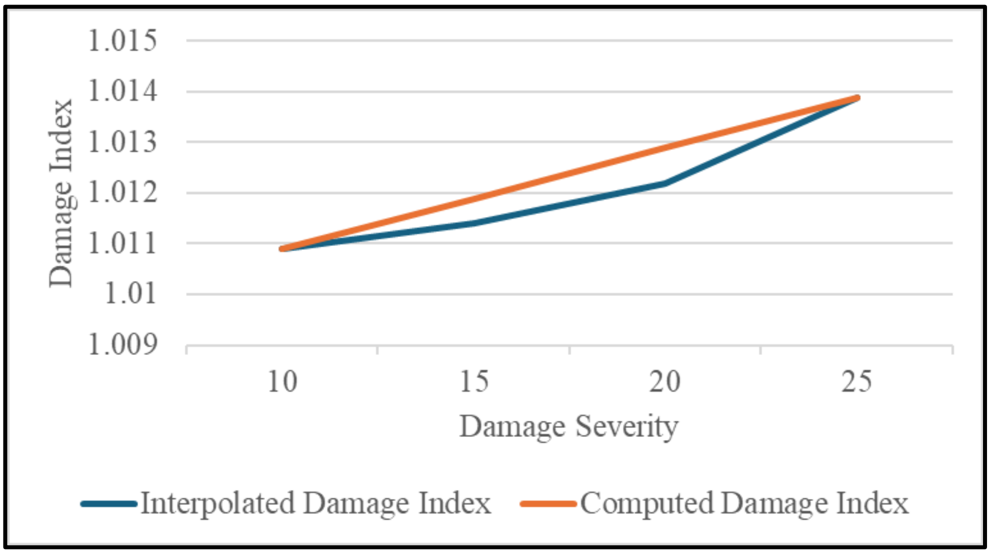

Figure 14: Comparison of computed and interpolated damage index.

From Table 4, the difference between the computed and interpolated DI is negligible, as the percentage difference is less than 1%. For severities ranging from 10% to 25%, interpolation was employed to generate the necessary damage index values, since training an ANN requires a substantial amount of data. Multiple datasets were generated to train the model using the neural network fitting tool in MATLAB. The DI was used as the input parameter for model training, while severity served as the output parameter. The dataset was divided into separate subsets for training, validation, and testing, as outlined in Table 5.

Table 5 : Datasets division for training, validation, and testing.

Data	**Samples**
Training	105
Validation	23
Testing	23

The training process produced regression results as illustrated in Figure 12, with an average coefficient of determination (R-squared) of 0.998. This high correlation between the predicted severity values and the actual severity values highlights the model's accuracy in capturing the underlying relationship between the input (DI) and the output (severity) variables.

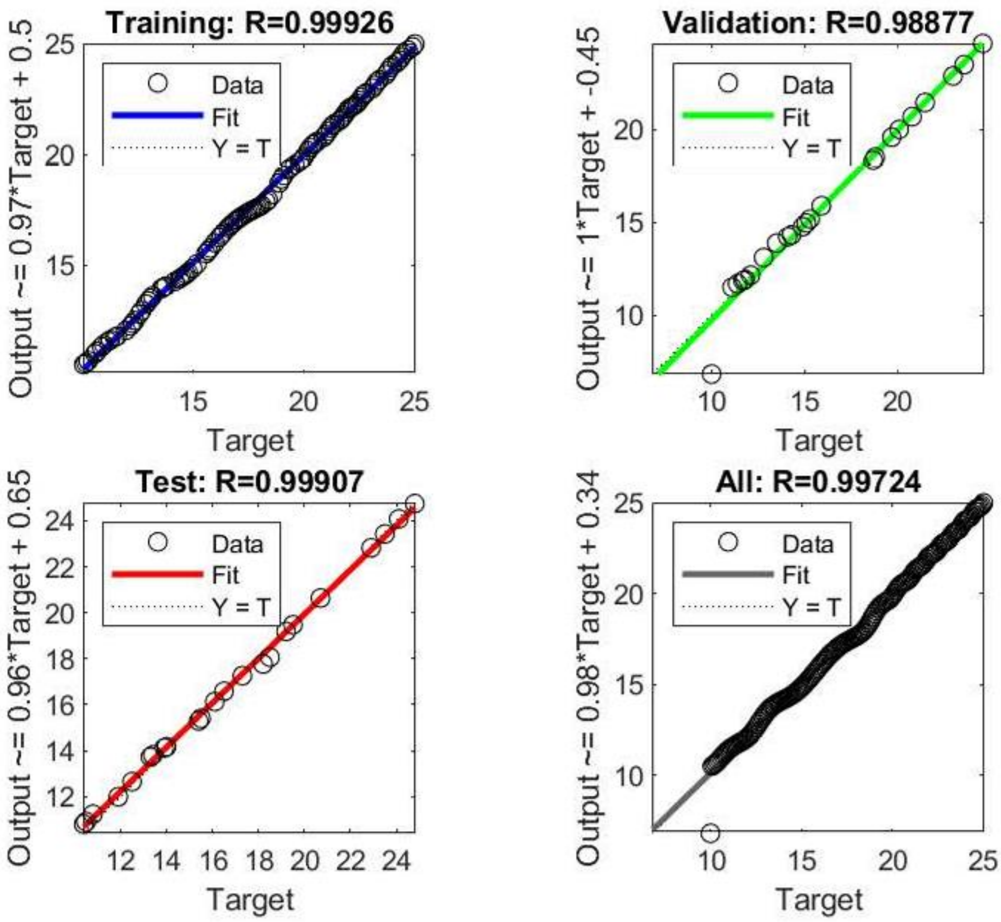

Figure 15: Regression plot of different data sets of ANN.

The use of distinct training, validation, and test datasets facilitated a comprehensive assessment of the model's performance across various data subsets, ensuring the reliability of the developed neural network model's predictive capabilities. The obtained regression results validate the effectiveness of the training approach, demonstrating the model's ability to accurately predict damage severity based on the provided input parameters.

4. Discussion

This study successfully developed and validated a novel two-stage process of identifying damage and quantifying that damage in terms of severity in the single span steel bridges, which was used on the FE model of the Alamosa Canyon Bridge. By employing the MSE-based DI technique initially for locating the damage, the ANN utilized this damage to quantify it in terms of severity. The proposed approach shows high precision in identifying damage locations for a different range of damage scenarios and severities. The suggested method demonstrates good accuracy in locating damage positions for a different range of damage scenarios and severities. The results shown by the proposed methodology also ensure that the applicability of this study in bridge health monitoring and contribute significantly to structural health monitoring, especially enhancing the accuracy, localization of damage, and its quantification in terms of severity in steel bridge structures.

The key findings of this research are as follows:

1. The MSE-based DI precisely localized the damage on the FE model of the Alamosa Canyon Bridge, with results showing the damage at specific locations of bridge segments for all scenarios.
2. Interpolated damage indices for severities ranging from 10% to 25% showed a small error of less than 1%, confirming the effectiveness of the interpolation used to extend the training dataset.
3. ANNs effectively quantify the severity-based damage with an average R-squared value of 0.998, showing a high correlation between actual severity and predicted values.
4. The proposed method is effective for structural health monitoring, promising more efficient and cost-effective bridge maintenance.

This methodology is purely based on simulation results without performing any practical or real-time data collection work on the target bridge. To advance the findings of this study, future research should focus on validating the proposed method across a range of bridge configurations and conditions, including varying deck configurations, material properties, and boundary conditions. Integration of real-time sensor data into the monitoring system should be explored to enhance detection accuracy and system responsiveness. Collaboration with bridge maintenance authorities and stakeholders is essential to facilitate the adoption and practical implementation of the system in real-world bridge management scenarios. Additionally, continuous refinement of the severity-based model is necessary to improve its predictive capabilities and adaptability to diverse bridge conditions and environments. Furthermore, due to the limited scope of the current study, confidence intervals or error bars were not included in the regression plot (Fig. 15); however, their inclusion can be considered in future work. Nonetheless, this is recognized as a valuable addition and is recommended for consideration in future work." Moreover, consideration should be given to scaling the implementation of this technology across a broader network of bridges to optimize infrastructure maintenance practices and enhance overall public safety. Physical testing in real-world scenarios is also needed to validate the system's performance and reliability.

5. Conclusions

The findings of this study differ from previous research by predicting damage severity using the MSE-based DI in the case of multi-damage scenarios for single-span steel bridges. According to past studies, the MSE-based DI effectively identifies damage locations but has contributed little to estimating the severity of the damage based on multi-damage scenarios for single-span steel bridges. This study addresses this gap by focusing on estimating the damage severity at identified locations, thereby presenting a novel contribution that effectively estimates damage severity with reduced computational effort. The comparative analysis demonstrates that the proposed method achieves desirable accuracy in both damage identification and severity prediction, offering a more efficient alternative to previously used methods.

However, there are a number of limitations; these include the fact that performance may vary in different ways on different bridges because of bridge-specific factors like variations in material values, boundary conditions and deck arrangements. In addition, this research was conducted on a simulation based-analysis and requires a wide-reaching field testing for its practical applicability.

Furthermore, the results of the conducted research on the suggested approach to damage detection induce the incorporation of the specified approach into the structural health monitoring procedures. The effectiveness of this methodology in the identification and forecast of damage of severity based using limited resources gives more time and cost-effective maintenance measures of bridges. This work holds a potentially positive outcome of incorporating the suggested method in structural testing-related guidelines and the codes of practice which could serve as a usable instrument in enhancing the stability and resistance of the steel bridge structure infrastructure.

Author Contributions: Conceptualization H.A.W., Z.U. and M.A.; methodology H.A.W., M.A., Z.U., and A.U.K.; visualization H.A.W., M.A., Z.U., and A.U.K.; validation H.A.W., M.A., Z.U., and A.U.K.; formal Analysis, M.A.; writing—original draft, H.A.W, Z.U. and M.A.; writing—review and editing H.A.W., Z.U. and M.A; All authors have read and agreed to the published version of the manuscript.

Funding: This research received no external funding.

Data Availability Statement: The data is available on reasonable request to the corresponding author.

Acknowledgments: This research involved technical Support from various engineering tools. The writing of this manuscript was accompanied by building finite element models within the Abaqus 2020 software, manipulation and analysis of data using scripts in the Python (version 3.12), and interpolation-based model calibration and regression-based interpretation of results with the help of MATLAB R2024a. The authors have critically checked and revised the work produced by these tools and takes total responsibility of the contents at hand.

Conflicts of Interest: The authors declare no conflict of interest.

Abbreviations

The following abbreviations are used in this manuscript:

SHM	Structural health monitoring
ANN	Artificial neural networks
MSE	Modal strain energy
DI	Damage Index
VBDD	Vibration-based damage detection
FE	Finite Element

BPNN	Back-propagation neural network
NLP	Multilayer perceptron
AV	Absolute value
MAE	Mean Absolute Error
LSTM	Long Short-Term Memory
MSE	Mean square error
VBM	Vibration based method

References

[1] E. J.; M. O'Brien Abdollah, "A mode shape-based damage detection approach using laser measurement from a vehicle crossing a simply supported bridge," *Struct Control Health Monit*, vol. 23, no. 10, pp. 1273–1286, 2016, doi: 10.1002/stc.1841.

[2] Y. T. Wang David; Chan Tommy H.T.; Nguyen Andy, "Damage detection in asymmetric buildings using vibration-based techniques," *Struct Control Health Monit*, vol. 25, no. 5, pp. e2148-NA, 2018, doi: 10.1002/stc.2148.

[3] S. O. Beskhyroun Toshiyuki; Mikami Shuichi, "Wavelet-based technique for structural damage detection," *Struct Control Health Monit*, vol. 17, no. 5, pp. 473–494, 2009, doi: NA.

[4] S. W. Beskhyroun Leon D.; Sparling Bruce F., "New methodology for the application of vibration-based damage detection techniques," *Struct Control Health Monit*, vol. 19, no. 8, pp. 632–649, 2011, doi: 10.1002/stc.456.

[5] S. E. R. Azam Ahmed; Linzell Daniel G., "Damage detection in structural systems utilizing artificial neural networks and proper orthogonal decomposition," *Struct Control Health Monit*, vol. 26, no. 2, pp. e2288-NA, 2018, doi: 10.1002/stc.2288.

[6] A. B.-N. Rahai Firooz; Esfandiari Akbar, "Damage assessment of structure using incomplete measured mode shapes," *Struct Control Health Monit*, vol. 14, no. 5, pp. 808–829, 2007, doi: 10.1002/stc.183.

[7] J. D. Li Ulrike; Xu You Lin; Samali Bijan, "Damage identification in civil engineering structures utilizing PCA-compressed residual frequency response functions and neural network ensembles," *Struct Control Health Monit*, vol. 18, no. 2, pp. 207–226, 2011, doi: 10.1002/stc.369.

[8] S. S. Das Purnachandra; Patro Sanjaya Kumar, "Vibration-based damage detection techniques used for health monitoring of structures: a review," *J Civ Struct Health Monit*, vol. 6, no. 3, pp. 477–507, 2016, doi: 10.1007/s13349-016-0168-5.

[9] H. R. A. Ahmadi Diana, "New damage index based on least squares distance for damage diagnosis in steel girder of bridge's deck," *Struct Control Health Monit*, vol. 25, no. 10, pp. e2232-NA, 2018, doi: 10.1002/stc.2232.

[10] K. D. C. Nguyen Tommy H.T.; Thambiratnam David, "Structural damage identification based on change in geometric modal strain energy-eigenvalue ratio," *Smart Mater Struct*, vol. 25, no. 7, pp. 075032-NA, 2016, doi: 10.1088/0964-1726/25/7/075032.

[11] J. M. W.; D. S. Brownjohn Alessandro; Xu You Lin; Wenzel Helmut; Aktan A. Emin, "Vibration-based monitoring of civil infrastructure: challenges and successes," *J Civ Struct Health Monit*, vol. 1, no. 3, pp. 79–95, 2011, doi: 10.1007/s13349-011-0009-5.

[12] W. Q. Fan Pizhong, "Vibration-based Damage Identification Methods: A Review and Comparative Study:" *Struct Health Monit*, vol. 10, no. 1, pp. 83–111, 2010, doi: 10.1177/1475921710365419.

[13] X. C. Yang Xianming, "Test verification of damage identification method based on statistical properties of structural dynamic displacement," *J Civ Struct Health Monit*, vol. 9, no. 2, pp. 263–269, 2019, doi: 10.1007/s13349-019-00331-0.

[14] P. J.; D. Cornwell Scott W.; Farrar Charles R., "APPLICATION OF THE STRAIN ENERGY DAMAGE DETECTION METHOD TO PLATE-LIKE STRUCTURES," *J Sound Vib*, vol. 224, no. 2, pp. 359–374, 1999, doi: 10.1006/jsvi.1999.2163.

[15] T. H.; L. Ooijevaar Richard; Warnet Laurent; de Boer A.; Akkerman Remko, "Vibration based Structural Health Monitoring of a composite T-beam," *Compos Struct*, vol. 92, no. 9, pp. 2007–2015, 2010, doi: 10.1016/j.compstruct.2009.12.007.

[16] F. F. Kopsaftopoulos Spilios D., "Vibration based health monitoring for a lightweight truss structure: experimental assessment of several statistical time series methods," *Mech Syst Signal Process*, vol. 24, no. 7, pp. 1977–1997, 2010, doi: 10.1016/j.ymssp.2010.05.013.

[17] A. G. Ruffels Ignacio; Karoumi Raid, "Model-free damage detection of a laboratory bridge using artificial neural networks," *J Civ Struct Health Monit*, vol. 10, no. 2, pp. 183–195, 2020, doi: 10.1007/s13349-019-00375-2.

[18] M. Z. Yang Hai; Telste Mike; Gajan Sivapalan, “Bridge damage localization through modified curvature method,” *J Civ Struct Health Monit*, vol. 6, no. 1, pp. 175–188, 2015, doi: 10.1007/s13349-015-0150-7.

[19] W. K. Xiong Bo; Tang Pingbo; Ye Jianshu, “Vibration-Based Identification for the Presence of Scouring of Cable-Stayed Bridges,” *J Aerosp Eng*, vol. 31, no. 2, pp. 04018007-NA, 2018, doi: 10.1061/(asce)as.1943-5525.0000826.

[20] N. K. Stubbs Jeong-Tae, “Damage Localization in Structures Without Baseline Modal Parameters,” *AIAA Journal*, vol. 34, no. 8, pp. 1644–1649, 1996, doi: 10.2514/3.13284.

[21] J.-T. S. Kim Norris, “Improved damage identification method based on modal information,” *J Sound Vib*, vol. 252, no. 2, pp. 223–238, 2002, doi: 10.1006/jsvi.2001.3749.

[22] A. A. Eraky Ahmed M.; Saad Alaa; Abdo Ayman, “Damage detection of flexural structural systems using damage index method - Experimental approach,” *Alexandria Engineering Journal*, vol. 54, no. 3, pp. 497–507, 2015, doi: 10.1016/j.aej.2015.05.015.

[23] H. W. T. Shih David; Chan Tommy H.T., “Vibration based structural damage detection in flexural members using multi-criteria approach,” *J Sound Vib*, vol. 323, no. 3, pp. 645–661, 2009, doi: 10.1016/j.jsv.2009.01.019.

[24] B. L. Samali Jianchun; Choi Fookchoon; Crews Keith, “Application of the damage index method for plate-like structures to timber bridges,” *Struct Control Health Monit*, vol. 17, no. 8, pp. 849–871, 2010, doi: 10.1002/stc.347.

[25] P. J. S.; S. Cruz R., “Performance of Vibration-Based Damage Detection Methods in Bridges,” *Computer-Aided Civil and Infrastructure Engineering*, vol. 24, no. 1, pp. 62–79, 2008, doi: 10.1111/j.1467-8667.2008.00546. x.

[26] N. L. Bonessio Giuseppe; Benzoni Gianmario, “Damage identification procedure for seismically isolated bridges,” *Struct Control Health Monit*, vol. 19, no. 5, pp. 565–578, 2011, doi: 10.1002/stc.448.

[27] C. R.; J. Farrar David A, “Comparative study of damage identification algorithms applied to a bridge: I. Experiment,” *Smart Mater Struct*, vol. 7, no. 5, pp. 704–719, 1998, doi: 10.1088/0964-1726/7/5/013.

[28] S. S. Park Norris; Bolton Robert; Choi Sang Hyun; Sikorsky Charles, “Field Verification of the Damage Index Method in a Concrete Box-Girder Bridge via Visual Inspection,” *Computer-Aided Civil and Infrastructure Engineering*, vol. 16, no. 1, pp. 58–70, 2001, doi: 10.1111/0885-9507.00213.

[29] N.; T. Jayasundara David; Chan Tommy H.T.; Nguyen Andy, “Vibration-based dual-criteria approach for damage detection in arch bridges,” *Struct Health Monit*, vol. 18, no. 5–6, pp. 2004–2019, 2019, doi: 10.1177/1475921718810011.

[30] Z. W. Zhou Leon D.; Sparling Bruce F., “Vibration-based detection of small-scale damage on a bridge deck,” *Journal of Structural Engineering*, vol. 133, no. 9, pp. 1257–1267, 2007, doi: 10.1061/(asce)0733-9445(2007)133:9(1257).

[31] H. W. T. Shih David; Chan Tommy H.T., “Damage detection in slab-on-girder bridges using vibration characteristics,” *Struct Control Health Monit*, vol. 20, no. 10, pp. 1271–1290, 2012, doi: 10.1002/stc.1535.

[32] I. F. Talebinejad Chad; Ansari Farhad, “Numerical Evaluation of Vibration-Based Methods for Damage Assessment of Cable-Stayed Bridges,” *Computer-Aided Civil and Infrastructure Engineering*, vol. 26, no. 3, pp. 239–251, 2010, doi: 10.1111/j.1467-8667.2010.00684. x.

[33] W. R. T. Wickramasinghe David; Chan Tommy H.T.; Nguyen Theanh, “Vibration characteristics and damage detection in a suspension bridge,” *J Sound Vib*, vol. 375, no. NA, pp. 254–274, 2016, doi: 10.1016/j.jsv.2016.04.025.

[34] A. K.; M. Garg D. Roy; Suresh Sundaram; Gopalakrishnan Srinivasan; Omkar S. N., “Estimation of composite damage model parameters using spectral finite element and neural network,” *Compos Sci Technol*, vol. 64, no. 16, pp. 2477–2493, 2004, doi: 10.1016/j.compscitech.2004.05.010.

[35] M.; K. Mehrjoo Naser; Moharrami Hamid; Bahreininejad Ardeshir, “Damage detection of truss bridge joints using Artificial Neural Networks,” *Expert Syst Appl*, vol. 35, no. 3, pp. 1122–1131, 2008, doi: 10.1016/j.eswa.2007.08.008.

[36] J.-J. Y. Lee Chung Bang, “Damage diagnosis of steel girder bridges using ambient vibration data,” *Eng Struct*, vol. 28, no. 6, pp. 912–925, 2006, doi: 10.1016/j.engstruct.2005.10.017.

[37] H. H. Xu Jagmohan, “Damage Detection in a Girder Bridge by Artificial Neural Network Technique,” *Computer-Aided Civil and Infrastructure Engineering*, vol. 21, no. 6, pp. 450–464, 2006, doi: 10.1111/j.1467-8667.2006.00449. x.

[38] J. G. Gu Mustafa; Wu Xiaoguang, “Damage detection under varying temperature using artificial neural networks,” *Struct Control Health Monit*, vol. 24, no. 11, pp. e1998-NA, 2017, doi: 10.1002/stc.1998.

[39] Z. X. T. Tan David; Chan Tommy H.T.; Razak H. Abdul, “Detecting damage in steel beams using modal strain energy-based damage index and Artificial Neural Network,” *Eng Fail Anal*, vol. 79, no. NA, pp. 253–262, 2017, doi: 10.1016/j.engfailanal.2017.04.035.

[40] A. H. Bagchi JagMohan; Xu Hongpo; Noman Ahmed S., “Model-Based Damage Identification in a Continuous Bridge Using Vibration Data,” *Journal of Performance of Constructed Facilities*, vol. 24, no. 2, pp. 148–158, 2010, doi: 10.1061/(asce)cf.1943-5509.0000071.

[41] A. L. Sabamehr Chaewoon; Bagchi Ashutosh, “System identification and model updating of highway bridges using ambient vibration tests,” *J Civ Struct Health Monit*, vol. 8, no. 5, pp. 755–771, 2018, doi: 10.1007/s13349-018-0304-5.

[42] U. L. Dackermann Jianchun; Samali Bijan, “Dynamic-Based Damage Identification Using Neural Network Ensembles and Damage Index Method:” *Advances in Structural Engineering*, vol. 13, no. 6, pp. 1001–1016, 2010, doi: 10.1260/1369-4332.13.6.1001.

[43] S. J. S.; R. Hakim H. Abdul, “Structural damage detection of steel bridge girder using artificial neural networks and finite element models,” *Steel & Composite structures*, vol. 14, no. 4, pp. 367–377, 2013, doi: 10.12989/scs.2013.14.4.367.

[44] Charles R. Farrar, Phillip J. Cornwell, Scott W. Doebling, and Michael B. Prime, “Structural Health Monitoring Studies of the Alamosa Canyon and I-40 Bridges,” Jul. 2000, doi: 10.2172/766805.

[45] H. A. Waqas, D. Su, and T. Nagayama, “Identification of sliding plate bridge bearing malfunction and its effects on bridge structure under service conditions,” *J Civ Struct Health Monit*, vol. 14, no. 4, pp. 947–961, Apr. 2024, doi: 10.1007/S13349-024-00764-2.